

Distinct transport regimes for two elastically coupled molecular motors - EPAPS

Appendices

Florian Berger, Corina Keller, Stefan Klumpp and Reinhard Lipowsky
Theory & Bio-Systems, Max Planck Institute of Colloids and Interfaces, 14424 Potsdam, Germany
 (Dated: February 28, 2012)

I. NETWORK DESCRIPTION OF TWO ELASTICALLY COUPLED MOTORS

In the following, we provide a detailed description of our microscopic model to calculate the motor pair parameters t_2 and v_2 . Both motors are attached to the cargo via elastic linkers. Because of the discrete stochastic stepping of the motors, a motor step leads to stretching or relaxation of the two linkers and thereby to a displacement of the cargo. When motors that start in the state, in which both linkers are relaxed, walk either towards each other or away from each other their linkers are stretched, see Fig.S1. We describe the cargo in the state space $(0) \dots (N)$ of the discrete extension of the linkers, see Fig.S2. In every state (i) the force F_i is exerted on one motor and the opposing force $-F_i$ on the other. These forces are calculated according to a force extension relation $F(x)$ that mimics the elastic linkers. In our study, we use a linear force extension relation. Since the elastic coupling generates an attractive force between the motors, we can choose N large enough, such that all results do not depend on N . In state (0) the linkers are relaxed. If one of the motors steps forward or backward the absolute extension of both linkers increases by the motor step size l and the cargo is in state (1) . For identical motors each linker is stretched by $x = l/2$. This stretching induces a strain force between the motors. One motor feels the force $F_1 = F(l/2)$ and the other motor feels the opposing force $-F_1 = -F(l/2)$. We denote transition rates for stretching of the linkers $\omega_s(i)$ and for relaxation $\omega_r(i)$. These transition rates are connected to the known force dependent forward stepping rates $\alpha(F)$ and backward stepping rate $\beta(F)$ of the single motors. When the cargo is in state (0) with both linkers relaxed, the force on each motor is zero, $F(0) = -F(0) = 0$. There are four possible pathways from state (0) to state (1) : either one of the motor can step forward or backward. Therefore, the transition rate from state (0) to state (1) reads

$$\omega_s(0) \equiv 2[\alpha(0) + \beta(0)]. \quad (\text{S.1})$$

For the other states $i > 0$ the transitions are governed by the rates

$$\omega_s(i) \equiv \alpha(F_i) + \beta(-F_i) \quad (\text{S.2})$$

$$\omega_r(i) \equiv \alpha(-F_i) + \beta(F_i) \quad (\text{S.3})$$

As a first approximation, we neglect back stepping, i.e. $\beta(F) = 0$ and relate the forward stepping rate to the simple piecewise linear force velocity relation

$$\mathcal{V}(F_i) \equiv \begin{cases} v & F_i < 0 \\ v(1 - F_i/F_s) & 0 \leq F_i < F_s \\ 0 & F_i \geq F_s, \end{cases} \quad (\text{S.4})$$

leading to the rates

$$\omega_s(0) \equiv 2v/l \quad (\text{S.5})$$

and for $i > 0$

$$\omega_s(i) \equiv (v/l)(1 - F_i/F_s), \quad (\text{S.6})$$

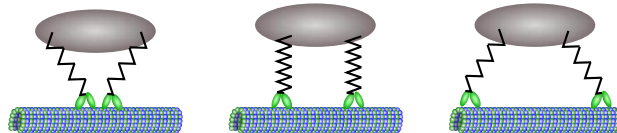


FIG. S1: Illustration of the extension of the motor linkers when the motors walk either towards each other or away from each other.

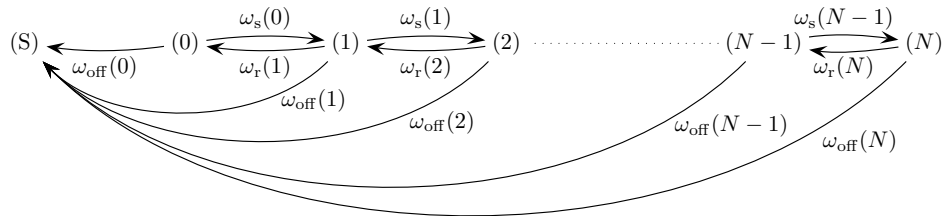


FIG. S2: Discrete state space describing the extension of the linkers. In state (0) the linkers are relaxed. The other states (i) correspond to the extension of the linkers by a distance $il/2$. Transitions between these states are described by extension rates ω_s or relaxation rates ω_r . Motors unbind with rates ω_{off} leading into the absorbing state (S).

$$\omega_r(i) \equiv v/l. \quad (\text{S.7})$$

To account for backward steps, we use the definition of the force velocity relation

$$\mathcal{V}(F) = l[\alpha(F) - \beta(F)] \quad (\text{S.8})$$

and of the ratio of forward to backward steps

$$q(F) = \frac{\alpha(F)}{\beta(F)}, \quad (\text{S.9})$$

which leads to

$$\alpha(F) = \frac{q(F)}{q(F) - 1} \frac{\mathcal{V}(F)}{l} \quad (\text{S.10})$$

and

$$\beta(F) = \frac{1}{q(F) - 1} \frac{\mathcal{V}(F)}{l}. \quad (\text{S.11})$$

In this way we relate the stepping rates of our model to experimental accessible quantities, the force velocity relation and the ratio of forward to backward steps, which for example has been measured for kinesin-1 [1].

Since motors are able to unbind, we add an absorbing state (S), in which only a single motor is active. Since it is not likely that both motors unbind exactly at the same time, there is a possible transition from every state (0) ... (N) to the state in which the cargo is transported by a single motor. These transitions are associated with the force dependent unbinding rates of the individual motors through

$$\omega_{\text{off}}(i) \equiv \epsilon_1(F_i) + \epsilon_1(-F_i) = \epsilon e^{|F_i|/F_d} + \epsilon e^{-|F_i|/F_d} = 2\epsilon e^{|F_i|/F_d}. \quad (\text{S.12})$$

Here we use the experimentally motivated relation $t_1(F) = 1/\epsilon_1(F) = t \exp(-F/F_d)$, but we note that any other relation, as well as other force-velocity relations could also be incorporated within this theoretical framework.

With this we complete our network description, see Fig. S2. Since we are interested in the quantities t_2 and v_2 , which are determined by the dynamics when both motors are active, we treat the state (S) as an absorbing state, see Fig. S2. In this general model we identify t_2 as the inverse of the mean time to absorption, which depends on the initial condition. We assume that, when one motor is bound the second motor initially binds in such a way that the linkers are relaxed. Averaged quantities like the mean time to absorption are usually obtained from time averages of the time dependent probability distribution of the 'open' network with the absorbing state. In ref. [2, 3] Hill introduced an elegant way to calculate such quantities by replacing the time average by an ensemble average. The basic idea is that upon reaching the absorbing state, the trajectories immediately re-start at the initial state. A network for such dynamics is obtained by eliminating the absorbing state and redirecting all arrows directed towards the absorbing state to the initial state, see Fig. S3. For such a closed network a meaningful steady state probability distribution P_i is determined from the solution of the steady state master equation,

$$\begin{aligned} \partial_t P_0 &= -[\omega_s(0) + \omega_{\text{off}}(0)]P_0 + \omega_r(1)P_1 + \sum_{j=0}^N \omega_{\text{off}}(j)P_j \\ \partial_t P_i &= \omega_s(i-1)P_{i-1} - [\omega_s(i) + \omega_r(i) + \omega_{\text{off}}(i)]P_i + \omega_r(i+1)P_{i+1} \quad \text{for } 0 < i < N \\ \partial_t P_N &= \omega_s(N-1)P_{N-1} - [\omega_r(N) + \omega_{\text{off}}(N)]P_N. \end{aligned} \quad (\text{S.13})$$

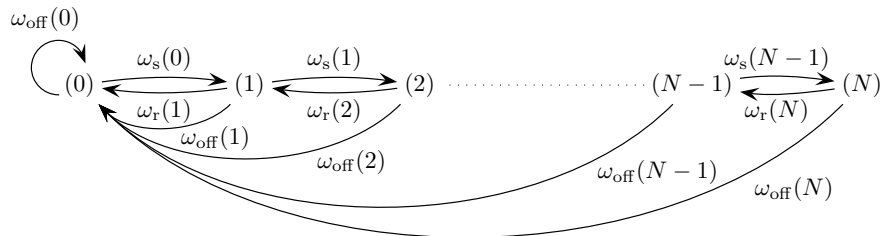


FIG. S3: Closed network of network in Fig. S2 obtained by redirecting all arrows that lead into the absorbing state back into the initial starting state (0).

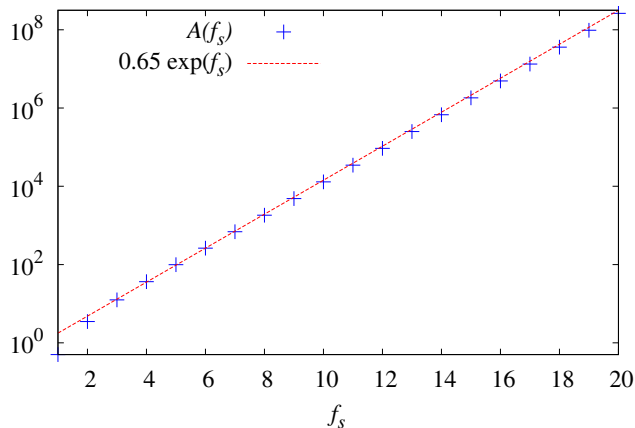


FIG. S4: Logarithmic plot of the sum $A(f_s)$ from Eq. (S.25) and the numerical approximation $0.65 \exp(f_s)$. The numerical prefactor $b \simeq 0.65$ is obtained from a least square fit of the function $b \exp(f_s)$ to the sum $A(f_s)$ for $f_s \in [1, 6]$.

Together with the normalization condition, this set of equations can be solved with a backward substitution, since P_N only depends on P_{N-1} . Here P_i is the probability of being in state (i) before absorption. This is equivalent to the time spent in state (i) divided by the mean time to absorption. Now, t_2 is given by the inverse probability current J into the absorbing state [4, 5],

$$t_2 = J^{-1} = \left(\sum_{i=0}^N \omega_{\text{off}}(i) P_i \right)^{-1} \quad (\text{S.14})$$

The mean velocity is obtained from averaging the force-velocity relations for both motors with the probability distribution before absorption,

$$v_2 \equiv \frac{1}{2} \sum_i [\mathcal{V}(iF_K) + \mathcal{V}(-iF_K)] P_i. \quad (\text{S.15})$$

II. DETAILED CALCULATION OF THE TIME SCALES

We obtain the crossover line between the different transport regimes by comparing three different times scales: the time scale for spontaneous unbinding $t_u \equiv 1/(2\epsilon)$ and the two time scales t_{F_d} and t_{F_s} it takes to generate forces larger than or equal to the detachment force and the stall force, respectively. For calculating the latter two times, we neglect unbinding. Hence the time t_{F_d} is the mean first passage time to end in state ($\lceil f_d \rceil$), when starting in state (0). Here the ceiling function ensures that the force in the target state is equal to or greater than F_d . This mean first passage time is given by

$$t_{F_d} \equiv \sum_{i=0}^{\lceil f_d \rceil - 1} \sum_{j=0}^i \frac{\omega_r(i) \omega_r(i-1) \dots \omega_r(j+1)}{\omega_s(i) \omega_s(i-1) \dots \omega_s(j+1) \omega_s(j)}, \quad (\text{S.16})$$

see [6]. We rewrite Eq. (S.16) using Eq. (S.5) - (S.7) and obtain

$$t_{F_d} = \sum_{i=0}^{\lceil f_d \rceil - 1} \left(\frac{\prod_{k=1}^i \alpha(-kF_K)}{2 \prod_{k=0}^i \alpha(kF_K)} + \sum_{j=1}^i \frac{\prod_{k=1+j}^i \alpha(-kF_K)}{\prod_{k=j}^i \alpha(kF_K)} \right) = \frac{l}{v} \sum_{i=0}^{\lceil f_d \rceil - 1} \left(\frac{1}{2 \prod_{k=0}^i (1 - \frac{k}{f_s})} + \sum_{j=1}^i \frac{1}{\prod_{k=j}^i (1 - \frac{k}{f_s})} \right). \quad (\text{S.17})$$

Note that this sum diverges for $f_d > f_s$, since the forces between the motors are bounded by the stall force F_s , and hence they never reach the detachment force if $F_d > F_s$.

The crossover between regimes (I) and (III), where unbinding is unaffected by the coupling, and the regimes (II) and (IV) with a reduced binding time is characterized by a crossover line that is defined by $t_{F_d} = t_u$, leading to

$$\frac{l}{v} \sum_{i=0}^{\lceil f_d \rceil - 1} \left(\frac{1}{2 \prod_{k=0}^i (1 - \frac{k}{f_s})} + \sum_{j=1}^i \frac{1}{\prod_{k=j}^i (1 - \frac{k}{f_s})} \right) = \frac{1}{2\epsilon}. \quad (\text{S.18})$$

This equation defines the implicit crossover line between the regimes $f_d(f_s)$. The numerical solution is displayed as the solid black lines in Fig. 2 of the main text. The steps in this function arise from the ceiling function in the upper limit of summation. We approximate the crossover line with a Michaelis-Menten like behavior

$$f_d(f_s) = \frac{f_d^* f_s}{f_d^* + f_s - 1}, \quad (\text{S.19})$$

that satisfies the constrain $f_d(1) = 1$. The saturation value f_d^* is obtained by taking the limit $f_s \rightarrow \infty$ in Eq. (S.18),

$$\lim_{f_s \rightarrow \infty} t_{F_d}(f_s) = \frac{l \lceil f_d \rceil^2}{2v} = \frac{1}{2\epsilon}. \quad (\text{S.20})$$

The left hand side of this equation is a discrete object, while the right hand side is a continuous object. Therefore, we determine the smallest value f_d^* for which $t_{F_d} \geq t_u$, leading to

$$f_d^* = \left\lceil \sqrt{\frac{v}{l\epsilon}} \right\rceil. \quad (\text{S.21})$$

Here, we see that f_d^* increases for increasing $v/l\epsilon$.

The time t_{F_s} is obtained in the same way as the time t_{F_d} , but with a different target state ($\lceil f_s \rceil$), in which the force is greater or equal to the stall force,

$$t_{F_s} = \frac{l}{v} \sum_{i=0}^{\lceil f_s \rceil - 1} \left(\frac{1}{2 \prod_{k=0}^i (1 - \frac{k}{f_s})} + \sum_{j=1}^i \frac{1}{\prod_{k=j}^i (1 - \frac{k}{f_s})} \right). \quad (\text{S.22})$$

The crossover line between the regimes (II) and (III) with a reduced velocity and the regimes (I) and (IV) with an unchanged velocity is given by $t_{F_s} \simeq t_u$, leading to

$$\frac{l}{v} \sum_{i=0}^{\lceil f_s \rceil - 1} \left(\frac{1}{2 \prod_{k=0}^i (1 - \frac{k}{f_s})} + \sum_{j=1}^i \frac{1}{\prod_{k=j}^i (1 - \frac{k}{f_s})} \right) \simeq \frac{1}{2\epsilon}. \quad (\text{S.23})$$

This equation is independent of the rescaled detachment force. However, solving this equation in a unique way is not straight forward, because f_s appears in the ceiling function in the upper limit of summation and in the denominator. To circumvent these issues, we define the crossover line as the smallest integer f_s^* for which $t_{F_s} \geq t_u$ holds. To show that f_s^* also increases with increasing $v/l\epsilon$, we rewrite t_{F_s} as

$$t_{F_s} = \frac{l}{v} A(f_s), \quad (\text{S.24})$$

where

$$A(f_s) \equiv \sum_{i=0}^{\lceil f_s \rceil - 1} \left(\frac{1}{2 \prod_{k=0}^i (1 - \frac{k}{f_s})} + \sum_{j=1}^i \frac{1}{\prod_{k=j}^i (1 - \frac{k}{f_s})} \right). \quad (\text{S.25})$$

From the numerical evaluation of this sum, we find that $A(f_s)$ can be approximate by $A(f_s) \simeq 0.65 \exp(f_s)$ for integer f_s , see Fig. S4. Therefore, the sum increases exponentially, i.e.,

$$A(f_s) \sim e^{f_s}. \quad (\text{S.26})$$

Using the definition of the crossover line, we derive the scaling of this line, as

$$f_s^* \sim \left\lceil \ln \frac{v}{2l\epsilon} \right\rceil \quad (\text{S.27})$$

In summary, the values f_d^* and f_s^* are increasing functions of $v/l\epsilon$, which is the single motor run length in units of the step size.

III. PARAMETERS FOR THE COMPARISON OF DIFFERENT MOTOR PAIRS

| parameter | kinesin-1 _{Bl} | kinesin-1 _{Di} | strong dynein | weak dynein | myosin V | myosin VI |
|---|-------------------------|-------------------------|---------------|-------------|-----------|-----------|
| stall force F_s [pN] | 6 [7, 8] | 7 [1, 9] | 7 [10] | 1.1 [11] | 2 [12] | 2 [12] |
| detachment force F_d [pN] | 3 [8] | 3 [8] | 0.75 [13] | 0.75 [13] | 4 [12] | 2.6 [12] |
| velocity v [$\mu\text{m/s}$] | 1 [1, 8] | 0.5 [14] | 0.65 [13] | 0.65 [13] | 0.38 [12] | 0.15 [12] |
| unbinding rate ϵ [s^{-1}] | 1 [8] | 0.61 [14] | 0.27 [13] | 0.27 [13] | 0.3 [12] | 0.25 [12] |
| step size l [nm] | 8 [1] | 8 [14] | 8 [10] | 8 [10] | 36 [12] | 36 [12] |

TABLE S1: Values of the single-motor parameters used to study the motor-motor interference of different pairs of elastically coupled motors.

| regimes | kinesin-1 _{Bl} | kinesin-1 _{Di} | strong dynein | weak dynein | myosin V | myosin VI |
|---------|-------------------------|-------------------------|------------------|--------------------------|------------------|------------------|
| (I) | $\kappa < 0.125$ | $\kappa < 0.125$ | $\kappa < 0.014$ | $\kappa < 0.027$ | $\kappa < 0.028$ | $\kappa < 0.037$ |
| (II) | $\kappa > 0.3$ | $\kappa > 0.35$ | - | $\kappa > 0.046$ | - | - |
| (III) | - | - | - | - | $\kappa > 0.028$ | $\kappa > 0.037$ |
| (IV) | $0.125 < \kappa < 0.3$ | $0.125 < \kappa < 0.35$ | $\kappa > 0.014$ | $0.027 < \kappa < 0.046$ | - | - |

TABLE S2: Ranges for the different transport regimes given as the coupling strength κ in pN/nm for different motor pairs with parameters from Table S1.

Table S1 summarizes the parameters for different types of motors, which are used to predict the behavior of motor pairs with different coupling strengths. For kinesin, we include two data sets, one based on the single molecule experiments from the Block lab [8], and one based on data for the kinesin construct used in the 2-kinesin-complex studied by the Diehl lab [9, 14]. Likewise, we include two data sets for dynein, as very different stall forces for dynein have been reported. We note, that for a qualitative study we use the same form of the force-velocity relation for all motors. Likewise, the form of the force dependent unbinding rate and of the force-extension relation for the elastic linkers are always the same, only with different parameters. However, our framework could be used to describe cargo transport by two molecular motors in more detail, as soon as more parameters and force dependencies from single molecule experiments for different motors are available.

By changing the coupling strength, different transport regimes can be accessed. In Table S2 we show the range of coupling strength in which the different regimes are obtained for different molecular motors.

IV. EFFECTS OF BACKWARD STEPPING AND OF THE FUNCTIONAL FORM OF THE FORCE VELOCITY RELATION

In this section, we discuss the effect of back stepping and different single motor force velocity relations on our results presented in the main text.

Backward stepping can easily be incorporated into our model, as shown above in section I. However, the dynamics of a motor pair is not strongly affected by back stepping for the following reason: For small forces, backward steps are very rare. Frequent back stepping only occurs for forces around or above the stall force. In a motor pair, if one motor

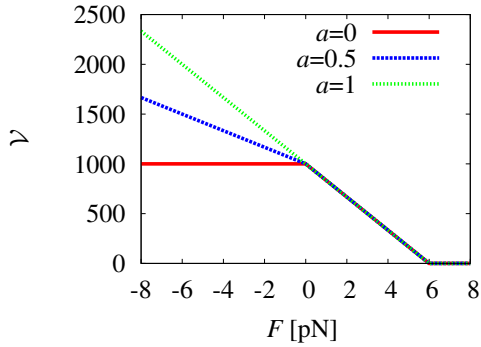


FIG. S5: Different force velocity relations of Eq. (S.28). The slope for assisting forces $F < 0$ can be varied via the parameter a

is under stall force, the other motor experiences an assisting force with a magnitude of the negative stall force. Under such conditions, the forward stepping rate for the motor under assisting force $\alpha(-F_s)$ is larger than the backward stepping rate for the motor under stall force $\beta(F_s)$. Therefore, even in the case of large strain forces between the motors, the most probable transition is a forward step by the motor under the negative force. Backward steps are included explicitly in the example with an empirical force velocity relation discussed below, which exhibit the same regimes as the model without back-steps in the main text.

Now, we vary the force dependence of the velocity for assisting forces, $F < 0$. In this range, experimental force-velocity curves from different studies exhibit the most pronounced discrepancies [15]. We use piecewise linear force velocity relations and vary the slope of the linear segment for $F < 0$ through the parameter a ,

$$\mathcal{V}(F_i) \equiv \begin{cases} v(1 - aF_i/F_s) & F < 0 \\ v(1 - F_i/F_s) & 0 \leq F_i < F_s \\ 0 & F_i \geq F_s \end{cases} \quad (\text{S.28})$$

see Fig. S5. For $a = 0$ the velocity is constant for assisting forces $F < 0$, whereas for $a = 1$ the slopes of the force velocity relation for the region $F < 0$ and the region $0 < F < F_s$ are the same.

Using the scaled forces f_s and f_d as described in the main text, we plot the scaled binding time t_2/t and scaled velocity v_2/v for different values of a , see Fig. S6. In addition, we calculate the crossover line between induced and spontaneous unbinding from the timescale argument $t_{F_d} = t_u$, see black lines in Fig. S6. For a larger slope of the force velocity relation, $a \rightarrow 1$, the region of induced unbinding (below the black line) is reduced. This can be understood from the following. For higher velocities under assisting forces the most probable transition is a forward step by the motor under negative force. Such a step reduces the distance between the motors and thus the strain force.

The case $a = 1$ represents an extreme case in which the velocity is constant, i. e., independent of the force scales, see Fig. S6(f). In this case, the regimes II and III with a reduced velocity disappear, because the strain between the motors does not affect the mean velocity for this form of the force velocity relation. This effect occurs generally for force velocity relations which are point symmetric with respect to $F = 0$, i. e., $\mathcal{V}(-F) - \mathcal{V}(0) = -[\mathcal{V}(F) - \mathcal{V}(0)]$. For such a force velocity relation the mean velocity of two active motors from Eq. (S.15) is independent of the strain force,

$$v_2 = \mathcal{V}(0) \sum_i P(F_i) = \mathcal{V}(0). \quad (\text{S.29})$$

Thus, the mean velocity is not reduced even if the strain force between the motor approaches the stall force. In such cases, the stall force does not provide an appropriate description of the decrease of the velocity (which in fact does not decrease at all). In other words, the strain force between the motors can be comparable to the stall force, without reducing the mean velocity of the cargo. In these extreme cases, the comparison of the timescales t_{F_s} and t_u does not reflect the crossover line between the two regimes, see blue lines in Fig. S6. However, the crossover between the weak coupling and enhanced unbinding regimes are correctly described by the comparison of t_{F_d} and t_u , see black lines in Fig. S6.

Finally, we consider an empirical force velocity relation obtained from a fit to the kinesin-1 data from [1] including back stepping. In [1], Carter and Cross have measured the force dependent ratio of forward and backward steps for kinesin-1, which could be approximated with

$$q(F) = q_0^{1 - \frac{F}{F_s}}, \quad (\text{S.30})$$

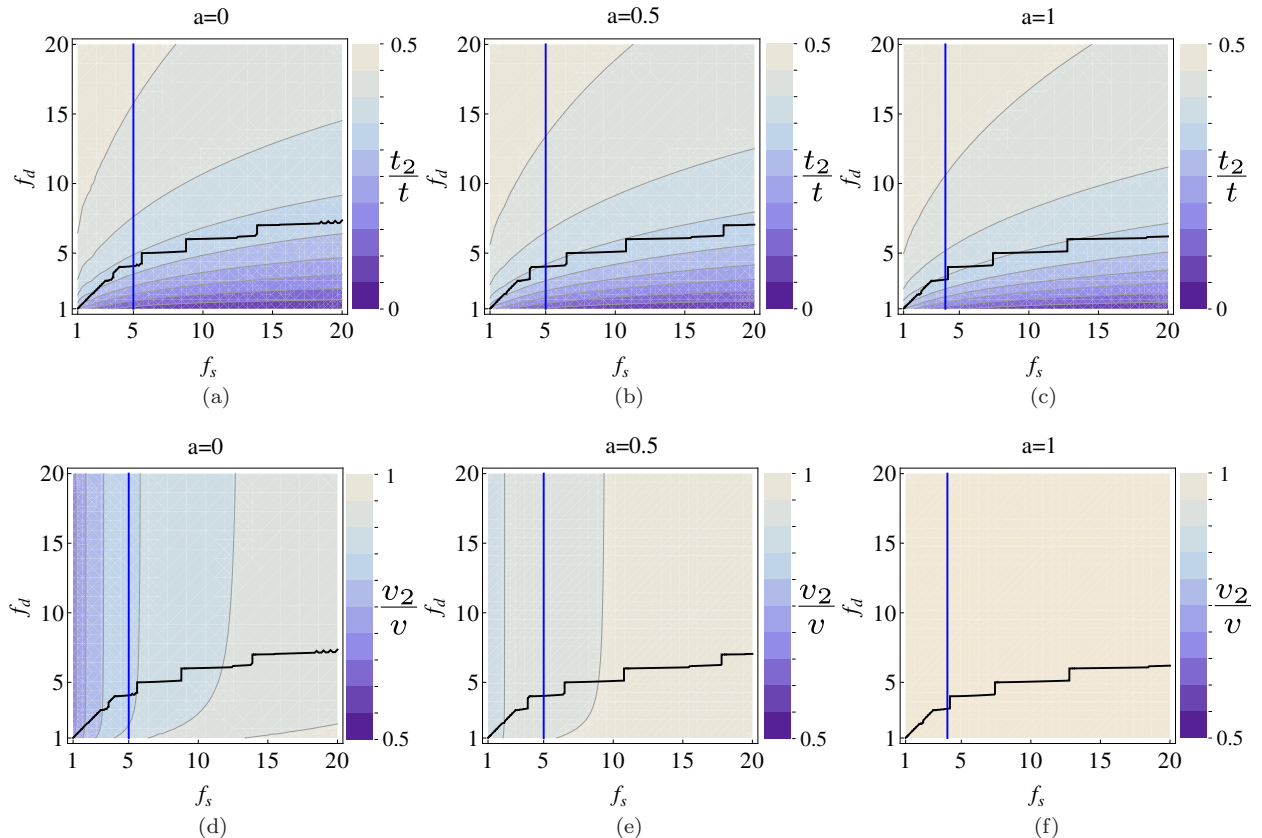


FIG. S6: The scaled binding time (a)-(c) and velocity (d)-(f) of two active motors as functions of the scaled forces f_s and f_d . The shape of the single motor force velocity relation is varied by the parameter a as shown in Fig.S5. The black line separates the regime of spontaneous unbinding (above the line) from the force-induced unbinding (below the line) determined as explained above. For $a = 1$, the force velocity relation is symmetric and v_2 is independent of the force and thus constant. The crossover line calculated with the time scale t_{F_s} is represented as the blue line.

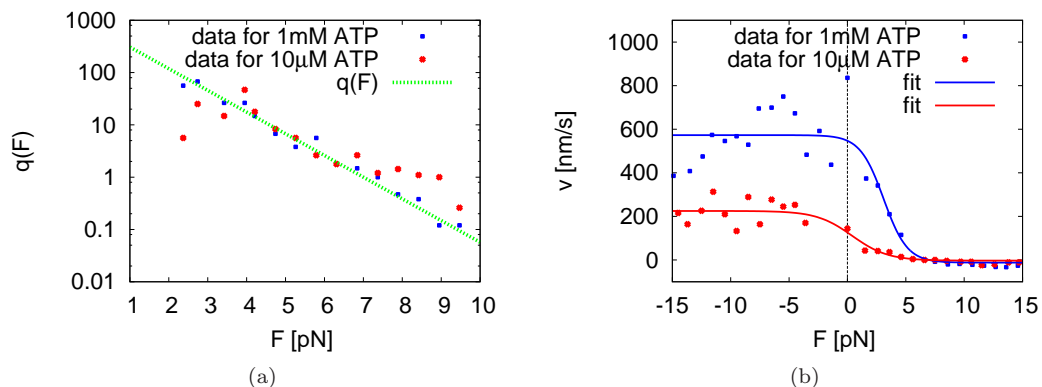


FIG. S7: Experimental data for kinesin-1 stepping taken from [1]. (a) Ratio of forward to backward stepping rates $q(F)$ as a function of load force F for different ATP concentrations. The line in the logarithmic plot is given by Eq. (S.30) with $q_0 \simeq 800$ and $F_s \simeq 7\text{pN}$ as suggested in [1]. (b) Force velocity relation for kinesin-1 for different ATP concentrations taken from [1]. The two lines are the force velocity relations from Eq. (S.31) and $F_s \simeq 7\text{pN}$, where we use a least square fit to obtain the parameters $v_0 \simeq 547\text{nm/s}$, $v_{\max} \simeq 573\text{nm/s}$ and $v_{\min} \simeq -12\text{nm/s}$ for 1mM ATP (blue) and $v_0 \simeq 126\text{nm/s}$, $v_{\max} \simeq 225\text{nm/s}$ and $v_{\min} \simeq -3\text{nm/s}$ for 10μM ATP (red).

where $q_0 \simeq 800$ independent of the ATP concentration, see Fig.S7(a). Furthermore, they obtained the force velocity relation for opposing and assisting forces for two different ATP concentrations, see Fig.S7(b). This data can be

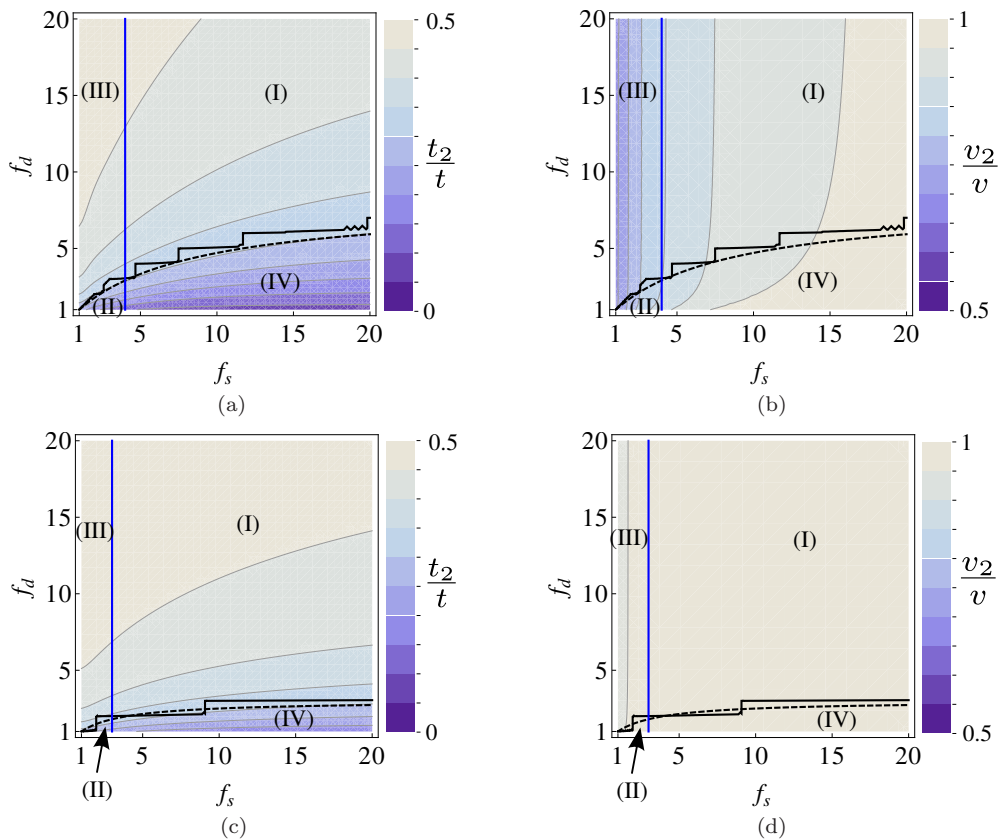


FIG. S8: Scaled binding time (a, c) and velocity (b, d) for two active kinesins taking back stepping into account. The single motor description is based on the force velocity relation and ratio of forward to backward steps, shown in Fig. S7 obtained by Carter and Cross in [1]. Plot (a) and (b) correspond to the data obtained with $[ATP]=1\text{mM}$ and (c) and (d) for the data with $[ATP]=10\mu\text{M}$. For the remaining parameters we use the kinesin values, $l \simeq 8\text{nm}$ and $\epsilon \simeq 1/\text{s}$. The crossover lines between the transport regimes are obtained as explained above, but taking backward stepping into account. The solid blue line separates the region with and without a reduced velocity, whereas the solid black line separates the region of spontaneous and force induced unbinding. The dashed lines correspond to the approximated crossover line. Slow motors with a low ATP concentration unbind before generating substantial strain forces, leading to reduced interference regimes (II), (III) and (IV), see (c) and (d).

described by

$$\mathcal{V}(F) = \frac{v_{\max} \frac{v_{\min}-v}{v-v_{\max}} + v_{\min} \left(\frac{v_{\max}}{v_{\min}} \frac{v_{\min}-v}{v-v_{\max}} \right)^{F/F_s}}{\frac{v_{\min}-v}{v-v_{\max}} + \left(\frac{v_{\max}}{v_{\min}} \frac{v_{\min}-v}{v-v_{\max}} \right)^{F/F_s}}. \quad (\text{S.31})$$

Here, we determine the maximal velocity v_{\max} , the minimal velocity v_{\min} and the velocity for zero force v from a least square fit to the measured data, see blue and red line in Fig. S7(b) and values in the caption. Using the ratio of Eq. (S.30) and the force velocity relation of Eq. (S.31), we determine the forward and backward stepping rates Eq. (S.10) and Eq. (S.11) for our network description.

Then, we calculate the the binding time t_2 and the velocity v_2 using our model including backward steps. These quantities are plotted in Fig. S8 as functions of the scaled forces f_s and f_d , together with the crossover lines. Fig. S8(a) and Fig. S8(b) show the results for high ATP concentration and exhibit qualitatively the same behavior as Fig. 2 of the main text obtained, where we have used the reduced description with a piecewise linear forces velocity relation and neglected back stepping. Fig. S8(c) and Fig. S8(d) show the corresponding results for the case of low ATP concentration. As explained in the main text, for lower ATP concentration, we expect a reduction of the interference, because strain forces are built up more slowly and motors unbind before generating substantial strain forces. Hence, the strong coupling, reduced velocity and enhanced unbinding region are smaller, as is indeed revealed by Fig. S8(c) and Fig. S8(d). Notice, that in this case, the crossover line predicted from the comparison of t_{F_s} and t_u is not very accurate, although it captures the qualitative behavior also for low ATP concentration. This is again due to the point

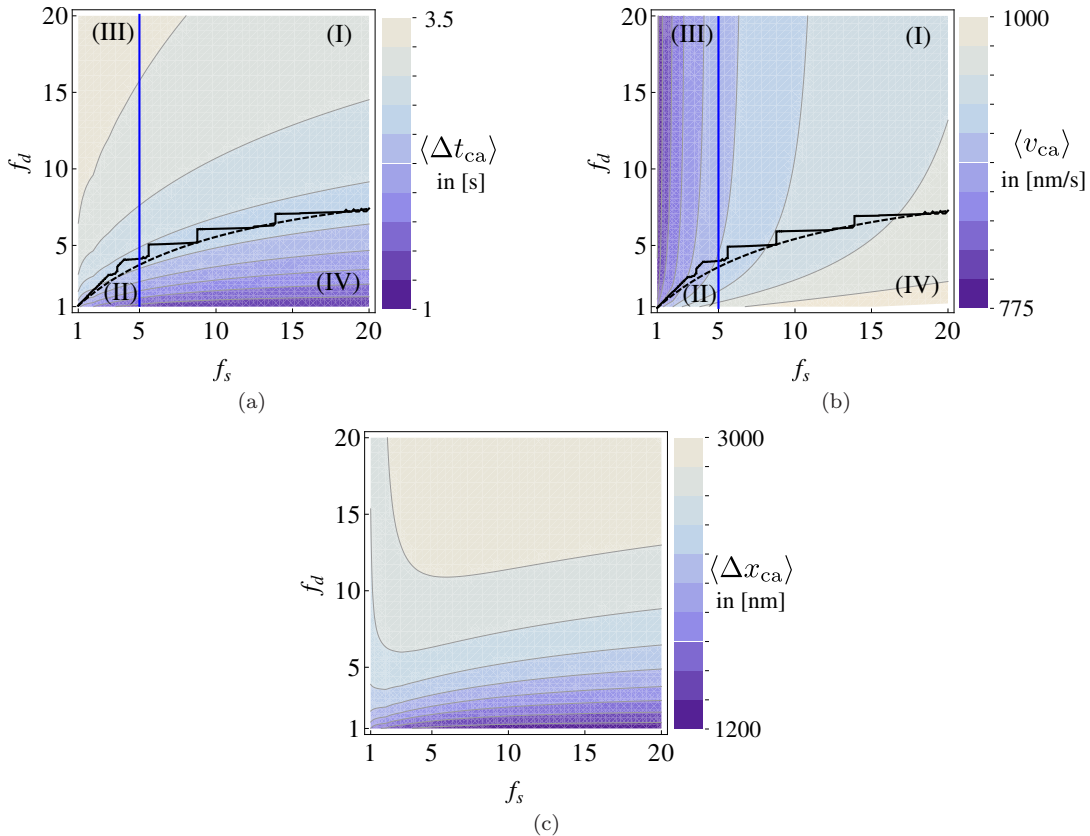


FIG. S9: Quantities describing an overall cargo run. The cargo is transported by two motors, which can unbind from and rebind to the filament. The single motors are described by the reduced model introduced in the main text with parameters $v/l \simeq 125/s$, $\epsilon \simeq 1/s$ with the additional binding rate $\pi \simeq 5/s$. Together with v_2 and t_2 of FIG. 2 of the main text, we plot in (a) the mean binding time of the cargo from Eq. (S.32), in (b) the mean velocity of the cargo from Eq. (S.34) and in (c) the mean run length of the cargo from Eq. (S.32) as functions of the scaled forces. The binding time and the velocity exhibit the four distinct transport regime even on this cargo level. The crossover lines are obtained as for Fig. 2 of the main text.

symmetry effect discussed above. Because of the slow stepping, the typical strain forces between the motors are rather small and the motors only sample the region of the force velocity relation close to $F = 0$, in which the force velocity relation is approximately point symmetric with respect to $F = 0$. As explained above, this symmetry decreases the force dependence of the mean velocity.

Taken together, the results of the main text do not substantially change when incorporating refinements such as backward stepping into the single motor description. The results obtained with the fitted force velocity relation for high ATP concentration are very similar to the one obtained with the reduced description. Conclusively, the reduced description captures the main characteristics of the force velocity relation for kinesin-1.

V. PROPERTIES OF AN OVERALL CARGO RUN

Our theoretical framework provides a way to calculate the characteristics t_2 and v_2 of 2-motor runs from the single motor parameters. Now, we use our results to calculate properties of an overall cargo run. An overall cargo run also includes the state, in which the cargo is transported only by one motor. The motors are able to unbind from and rebind to the filament. A general framework has been established to describe cargo transport by several motors [16]. Specifically, the binding time of the cargo to the filament is given by

$$\langle \Delta t_{ca} \rangle \equiv \frac{\pi + \epsilon_2}{\epsilon_1 \epsilon_2}, \quad (\text{S.32})$$

the mean run length of the cargo by

$$\langle \Delta x_{ca} \rangle \equiv \frac{\pi v_2 + \epsilon_2 v_1}{\epsilon_1 \epsilon_2}, \quad (\text{S.33})$$

and the mean velocity by

$$\langle v_{ca} \rangle \equiv \frac{\langle \Delta x_{ca} \rangle}{\langle \Delta t_{ca} \rangle} = \frac{\pi v_2 + \epsilon_2 v_1}{\pi + \epsilon_2}. \quad (\text{S.34})$$

In these expressions, ϵ_1 is the single motor unbinding rate, $\epsilon_2 = 1/t_2$ is the inverse binding time of two active motors, π is the binding rate of a motor, $v_1 = v$ is the velocity of one active motor and v_2 is the mean velocity of two active motors. All these quantities can thus be calculated from the single motor parameters, the 2-motor run characteristics t_2 and v_2 that we determined in the main text and one additional parameter, the binding rate π . All these quantities are plotted in Fig. S9 as functions of the scaled forces f_s and f_d using $v \simeq 1\mu\text{m/s}$, $\epsilon_1 \simeq 1/\text{s}$ and $\pi \simeq 5$ [17]. Inspection of the binding time and the velocity shows that the four different transport regimes can also be identified on the cargo level and agree well with the crossover lines estimated from the timescale arguments given above. In the weak coupling region, the mean run length is more than double the single motor run length $v_1/\epsilon_1 \simeq 1\mu\text{m}$, as expected for non interacting motors.

-
- [1] N. J. Carter and R. A. Cross, *Nature* **435**, 308 (2005).
 - [2] T. L. Hill, *Proc. Natl. Acad. Sci. U.S.A.* **85**, 2879 (1988).
 - [3] T. L. Hill, *Proc. Natl. Acad. Sci. U.S.A.* **85**, 4577 (1988).
 - [4] T. L. Hill, *Proc. Natl. Acad. Sci. U.S.A.* **85**, 3271 (1988).
 - [5] F. Berger, M. J. I. Müller, and R. Lipowsky, *Europhys. Lett.* **87**, 28002 (2009).
 - [6] N. G. van Kampen, *Stochastic processes in physics and chemistry* (North-Holland, Amsterdam, 1981).
 - [7] K. Svoboda and S. M. Block, *Cell* **77**, 773 (1994).
 - [8] M. Schnitzer, K. Visscher, and S. Block, *Nat. Cell. Biol.* **2**, 718 (2000).
 - [9] D. K. Jamison, J. W. Driver, A. R. Rogers, P. E. Constantinou, and M. R. Diehl, *Biophys. J.* **99**, 2967 (2010).
 - [10] S. Toba, T. M. Watanabe, L. Yamaguchi-Okimoto, Y. Y. Toyoshima, and H. Higuchi, *PNAS* **103**, 5741 (2006).
 - [11] R. Mallik, B. C. Carter, S. A. Lex, S. J. King, and S. Gross, *Nature* **427**, 649 (2004).
 - [12] M. Y. Ali, G. G. Kennedy, D. Safer, K. M. Trybus, H. Lee Sweeney, and D. M. Warshaw, *Proc. Natl. Acad. Sci. U.S.A.* **108**, E535 (2011).
 - [13] M. J. I. Müller, S. Klumpp, and R. Lipowsky, *Proc. Natl. Acad. Sci. U.S.A.* **105**, 4609 (2008).
 - [14] A. R. Rogers, J. W. Driver, P. E. Constantinou, D. K. Jamison, and M. R. Diehl, *Phys. Chem. Chem. Phys.* **11**, 4882 (2009).
 - [15] M. J. I. Müller, *Ph.D. Thesis: Bidirectional transport by molecular motors* (University of Potsdam, 2008).
 - [16] S. Klumpp and R. Lipowsky, *Proc. Natl. Acad. Sci. U.S.A.* **102**, 17284 (2005).
 - [17] J. Beeg, S. Klumpp, R. Dimova, R. S. Gracià, E. Unger, and R. Lipowsky, *Biophys. J.* **94**, 532 (2008).